Earthquakes and Structures, *Vol. 10, No. 2 (2016) 463-482*
DOI: http://dx.doi.org/10.12989/eas.2016.10.2.463

Seismic performance of a wall-frame air traffic control tower

Hossein Moravej[1a], Mohammadreza Vafaei[*2] and Suhaimi Abu Bakar[1b]

[1]*Faculty of Civil Engineering, Universiti Teknologi Malaysia, Johor, Malaysia*
[2]*Centers for Forensic Engineering, Faculty of Civil Engineering, Universiti Teknologi Malaysia, Johor, Malaysia*

(Received January 25, 2015, Revised December 8, 2015, Accepted December 11, 2015)

Abstract. Air Traffic Control (ATC) towers play significant role in the functionality of each airport. In spite of having complex dynamic behavior and major role in mitigating post-earthquake problems, less attention has been paid to the seismic performance of these structures. Herein, seismic response of an existing ATC tower with a wall-frame structural system that has been designed and detailed according to a local building code was evaluated through the framework of performance-based seismic design. Results of this study indicated that the linear static and dynamic analyses used for the design of this tower were incapable of providing a safety margin for the required seismic performance levels especially when the tower was subjected to strong ground motions. It was concluded that, for seismic design of ATC towers practice engineers should refer to a more sophisticated seismic design approach (e.g., performance-based seismic design) which accounts for inelastic behavior of structural components in order to comply with the higher seismic performance objectives of ATC towers.

Keywords: ATC tower; performance-based design; equivalent static analysis; response spectrum analysis; nonlinear time history analysis; seismic performance levels

1. Introduction

Airports are among vital infrastructures that should be endured totally functional during and after urban disaster such as earthquakes. Immediately after strong ground motions, carriage requests from damaged areas develop tremendously. A seismically designed airport can comply with such huge requests and mitigate significantly post-earthquake problems (Roark *et al*. 2000). ATC towers are among the most tactical and essential structures in all airports such that each airport needs one or more ATC tower in order to remain functional. Each entrance to or exit from airports should be monitored by ATC towers to avoid catastrophic incidents.

Vafaei *et al*. (2013) found dynamic behavior of ATC towers differ from chimneys and stacks on account of the concentrated mass of the observation and service rooms situated at the top of the tower. Contrary to reversed pendulum structures, in which the concentrated mass has governing

∗Corresponding author, Ph.D., E-mail: m.reza.vafaei@gmail.com
[a]Graduate student, E-mail: hosseinmoravej@yahoo.com
[b]Ph.D., E-mail: suhaimibakar@utm.my

http://www.techno-press.com/journals/eas&subpage=7 ISSN: 2092-7614 (Print), 2092-7622 (Online)

role in the dynamic behavior, in ATC towers, the mass of the horizontal load resistance system (usually made of reinforced concrete) has a notable influence on the dynamic responses. This means that, it is common to find a combination of both dynamic features that contribute to the dynamic behavior of ATC towers.

In spite of significant role that ATC towers play in the functionality of airports, only few researchers have studied seismic performance of these structures. Muthukumar and Sabelli (2013) studied seismic performance of a 67 m high ATC tower located in San Francisco International Airport through the performance-based seismic design approach. The structural system of the tower consisted of a cast-in-place reinforced concrete cylinder which was post-tensioned to act as a self-centering mechanism and reduce residual seismic drifts. At the Design Basis Earthquake (DBE) level, the performance goal was set as Immediate Occupancy (IO) level while at the Maximum Considered Earthquake (MCE) the performance goal was selected to be Collapse Prevention (CP). They concluded that although the tower exceeded the code-based height limitation for concrete shear wall system, the seismic behavior of the tower satisfied the performance objectives.

In another study, Vafaei *et al*. (2013) evaluated the seismic performance of Kuala Lumpur International Airport (KLIA) ATC tower. The tower was a 120 m high cast-in-place concrete shear wall structure. They employed a set of linear and nonlinear analysis to study seismic behavior of the tower. The obtained results revealed that linear analysis underestimated base shear, drifts and overturning moments when compared to nonlinear analyses. It was also found that pushover analysis may not be a suitable technique to evaluate seismic demands of such a tall ATC tower. Finally, they concluded that, the pile-foundation-structure interactions should be included in the Finite Element (FE) model in order to inhibit underestimation of seismic demands in the mid-height of the tower.

Wilcoski and Heymsfield (2002) worked on the seismic performance and rehabilitation of type L Federal Aviation Administration (FAA) ATC towers in the San Carlos airport, California. The type L towers consisted of four inverted L-shaped reinforced concrete members that framed together at the top of towers. The cabin structure was a moment resistance steel frame. The performance objective at the MCE was considered to be Life Safety (LS). They employed linear response spectrum analysis in their study. It was found that due to large deflections in cabin, towers could not achieve to LS level. Therefore, it was decided to stiffen and strengthen cab columns by welding cover plates on both interior and exterior faces.

Eshghi and Farrokhi (2003) evaluated seismic vulnerability of a 67 m high ATC tower located in Tehran, Iran. The structural system of the tower consisted of four hollow reinforced concrete boxes which were connected together via 25cm thick concrete slabs along the height of the tower. Response spectrum analysis together with Pushover analysis was employed for the vulnerability study. The obtained results indicated that slabs were the most vulnerable structural component and since they did not provide enough out of plan bending stiffness, the reinforced concrete boxes responded to lateral loads individually.

A review of the literature shows that, seismic design and performance of ATC towers have been a challenging matter for structural engineers. On the one hand, seismic performance level of ATC towers is remarkably higher than normal buildings because of the major role that they play in the rescue after seismic incidents. On the other hand, lack of informative guidelines and instructions for the seismic assessment and design of ATC towers can result in the improper usage of current building codes. Roark *et al*. (2000) presented this problem is deliberated until present, so more research is required to propose special guidelines for seismic design and performance assessment of ATC towers.

In this study, seismic vulnerability of the ATC tower of Urmia International Airport (Iran) was studied through linear and nonlinear analysis. The main objective of this study is to evaluate the seismic performance of a wall-frame ATC tower, which is designed and detailed in accordance with the conventional force-based concept, through the frame work of performance-based seismic design. This study addresses shear force and moment distribution between the concrete wall and steel frame of the tower and compares the results obtained from linear and nonlinear time history analyses when the tower is subjected to seismic loads. Meanwhile, the displacement demand of the tower obtained from inelastic analysis is compared with the prediction of employed seismic design code in order to evaluate accuracy of the force-based method in estimating displacement demand. Although the outcome of this study cannot be generalized for all ATC towers, it can help practice engineers to design such structures with more insight about seismic behavior of ATC towers.

2. Selected ATC Tower

The selected ATC tower is located in Urmia International Airport, Iran. Fig. 1 displays a schematic view of this tower. As can be seen from this figure, the structural system of this tower comprises of a steel Moment Resistance Frame (MRF) which is supported by two concrete cores. The outer core is connected to the MRF through circular beams and columns. The inner core is connected to the MRF via radial beams that are designed to support stairs. The inner and outer cores rise 11.68 m and 22.21 m above foundation level, respectively. The total height of the tower is 30.17 m. It can be seen that observation and equipment rooms rely only on the MRF. A slab with the thickness of 10 cm covers floors of observation and equipment room. The thickness of

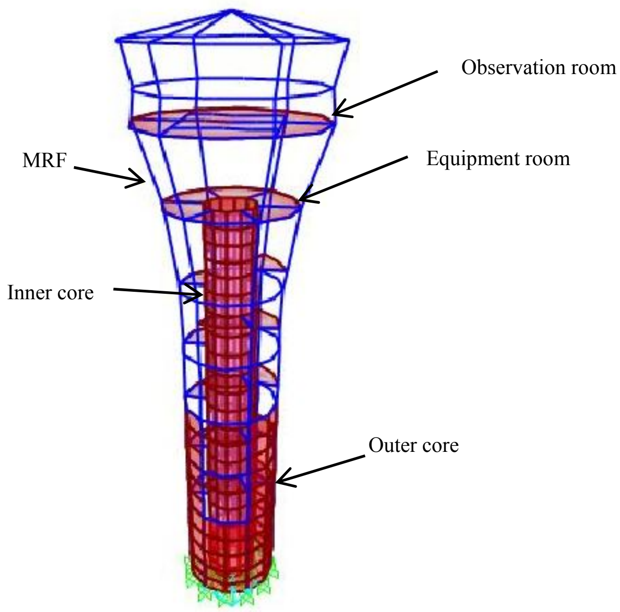

Fig. 1 Schematic view of the selected tower

Table 1 Reinforcement ratio of concrete cores

Wall Type	Height (m)		Reinforcement Ratio (%)	
	from	to	Horizontal	Vertical
External Core	0	11.68	0.7	2.1
Internal Core	0	11.68	0.9	2.1
Internal Core	11.68	22.21	0.9	1.4

Table 2 Size of columns

Levels		Width×height×Thickness (cm)
from (m)	to (m)	
0	22.2	30x30x1.5
22.21	25.84	30x30x2.5
25.84	29.07	20x20x1.2
29.07	30.17	30x20x0.8

Table 3 Size of circular beams

Level (m)	Height×Flange width×Thickness (cm)
5.20	30×20×1.5
8.44	30×20×0.8
11.68	30×20×1.5
14.92	30×20×1.5
18.16	35×25×1.2
22.21	35×25×1.5
25.84	35×25×1.5
27.24	30×20×0.8
29.07	35×20×1.5

concrete walls all along the height of tower is 0.3 m. All beam-to-column connections are fixed except for radial beams that have pin connections. The MRF consists of six columns with box-shaped cross sections. All beams have I-shaped cross sections. Table 1 displays the change in the reinforcement ratios of concrete cores. Tables 2 and 3 shows the size of beams and columns used in the MRF. It should be mentioned that the tower settles on a 15 m×15 m mat foundation with the thickness of 1.5 m. Due to the rigidity of the foundation, it was assumed that columns and concrete cores have fixed supports and soil-structure interactions were not included in the finite element model. It is worth mentioning that, design and detailing of the concrete walls and MRF were carried out in accordance with the requirements of American Concrete Institute (ACI) (ACI 318-99, 1999) and American Institute of Steel Construction (AISC) (AISC ASD89, 1989), respectively. The following load combinations were used for the design of concrete walls. In the load combination, (EL) stands for seismic load, (DL) and (LL) represent dead and live loads, respectively

$$1.4DL \tag{1}$$

$$1.4DL+1.7LL \tag{2}$$

$$0.9DL \pm 1.3*1.1EL \tag{3}$$

$$0.75(1.4DL+1.7LL \pm 1.7*1.1EL) \tag{4}$$

For the design of MRF the following load combinations were used

$$DL \tag{5}$$

$$DL+LL \tag{6}$$

$$DL+LL \pm EL \tag{7}$$

3. Seismic analysis

3.1 Finite element model of the tower

The inelastic behavior of reinforced concrete shear walls can be taken into account through two different techniques. In the first method, the inelastic behavior of concrete shear walls is characterized by stick models using continuous fiber elements while in the second approach discrete plastic hinges are employed. The former assumes that all cross sections are cracked and the tensile strength of the concrete and the tension stiffening effect are neglected. On the other hand, the second technique allows the analyst to directly model the effective stiffness of concrete walls and explains the effects of tension stiffening which considered by the publications (Goyal and Maiti 1997, Wilson 2003). It is worth mentioning that the second approach has been widely employed by researchers to model the inelastic behavior of concrete wall structures (Chen *et al*. 2010, Zekioglu *et al*. 2007, Değer *et al*. 2014, Mwafy *et al*. 2014).

The inelastic response of steel frames can be simulated via either the fiber elements or plastic hinge methodology. The fiber elements technique leads to the maximum accuracy whereas the plastic hinge approach agrees to a considerable simplification. In the first method, beams or columns are divided into many finite elements and the cross section of each element is modelled by fibers of which the stress-strain relationships are developed by the analysts (Kitipornchai *et al*. 1988, Pi and Trahair 1994, Izzuddin and Smith 1996, Foley and Vinnakota 1999, Teh and Clarke 1999, Jiang *et al*. 2002, McKenna *et al*. 2000, Li *et al*. 2014, Li *et al*. 2013, Shahidi *et al*. 2014). The fiber elements method is able to model the distribution of plasticization all over the cross-section and along the member length. Although the result of this technique is more accurate, it is recognized to be computationally intensive. In the second technique, inelastic response of beams and columns is modelled by plastic hinges that are normally lumped at both ends of elements. The clear benefit of this technique is that it is simple in formulation as well as application, and minimum elements are required to model members. In addition, it is able to reach to results that are correct enough for practical design (Al-Bermani and Kitipornchai 1990, Chan and Zhou 1998, Liew *et al*. 2000, Kim *et al*. 2001).

In this study, fiber elements were used to account for the inelastic behavior of concrete shear walls. Meanwhile, a brief comparison study was also performed to investigate the difference between results of discrete hinge method and the employed fiber technique. Linear and nonlinear material properties used to define fiber elements are presented in Tables 4 and 5, respectively. An unconfined stress-strain relationship was selected to be used for concrete fibers because no special detailing was employed to satisfy confinement condition. No tensile strength was considered for concrete fibers. The shear behavior of concrete fibers was simulated as elastic because of low shear demands observed for concrete walls during inelastic analyses. For reinforcement fibers stress-strain curve was defined as an elastic-perfectly-plastic (E-P-P) curve in which the strain hardening is ignored. This model also assumed a symmetrical behavior for reinforcements under tensile and comparison loads. Figs. 2(a) and 2(b) display the employed stress-strain relationship for concrete and reinforcement fibers, respectively. It should be mentioned that the values shown in Table 5 have been selected based on the recommendations of FEMA 356 (FEMA, 2000). Fig. 3 displays the generalized force-deformation relationship that is used for simulating inelastic behavior of beams and columns. FEMA 356 (FEMA 2000) recommendations along with cross-sectional properties of beams and columns were employed to define the required parameters in this figure. In the FE model, the inelastic behavior of beams and columns were taken into account by assigning plastic hinges to the beginning and end of elements.

As mentioned earlier, soil-structure interaction was not included in the FE model. However, P-delta effects were considered in the analyses. In addition, since the seismic demands of slabs were lower than their shear and flexural capacities, in the FE model they were simulated as an elastic element. The finite element model of the tower was established in SAP 2000 v15 (Computers and Structures 2013) software. This software has been employed by practice engineers for the design of different types of structures and its capability for simulating inelastic behavior of structures is verified by several studies. (Panneton *et al.* 2006, Orakcal *et al.* 2004, Rad and Adebar 2009)

Fig. 4 depicts the first, third and fifth mode shapes of the tower. The fifth mode shape displays a significant bending at the level of equipment room where the tower relies only on the MRF. This special dynamic characteristic of the tower indicates that, at this level, seismic demands in columns should experience a sudden increase. As reflected in Table 2, at the level of equipment room, the thickness of columns has been increased in order to comply with the additional seismic demands. Table 6 shows natural periods along with modal mass participating ratios in translational (U(x) and U(y)) and rotational (R(z)) directions. A significant contribution of rotational masses can be seen together with translational masses. Since the tower's mass has almost a symmetrical configuration all along the height, such combination of bending and torsional dynamic behavior can be attributed to the changes in the towers' stiffness. The main reason for such changes is the large openings that have been considered for the entrances of the lift along the height of the inner core. In order to consider this complex dynamic behavior into account, the first 35 mode shapes of the tower were included in the dynamic analyses. Consideration of the first 35 modes shapes assured attaining to 90% mass participation ratio for both principal directions as it is required by design codes (e.g., ASCE/SEI 7-10, 2010).

Table 4 Linear material properties of concrete and reinforcements

Material	Modulus of Elasticity	Poisson's Ratio	Compressive Strength	Yield Strength
Concrete	25400 (N/mm^2)	0.2	28 (N/mm^2)	-
Reinforcements	199940 (N/mm^2)	0.3	-	400 (N/mm^2)

Table 5 Nonlinear modeling parameters for concrete and reinforcements

	Ultimate Compressive Strain	Ultimate Tensile Strain
Concrete	0.005	-
Reinforcements	0.02	0.05

Table 6 Natural periods and modal participating mass ratios

Mode shape	Period (sec.)	U(x)	U(y)	R(z)
1st	0.69	1.3%	44%	21%
2nd	0.68	45%	1.2%	9.2%
3rd	0.36	0.01%	0.0	23%
4th	0.26	18%	0.1%	5.1%
5th	0.25	0.1%	17%	5.1%

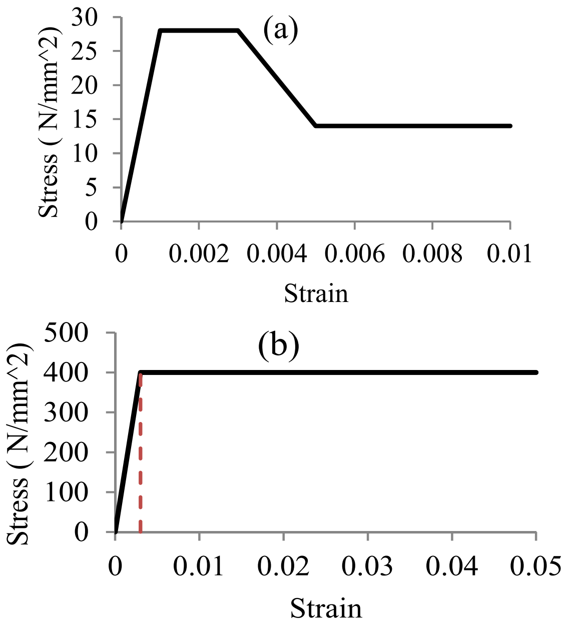

Fig. 2 (a) stress-strain relationship of concrete (b) stress-strain relationship of reinforcements

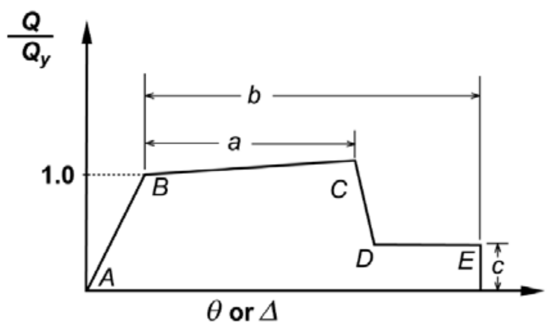

Fig. 3 The generalized force-deformation relationship employed for plastic hinges

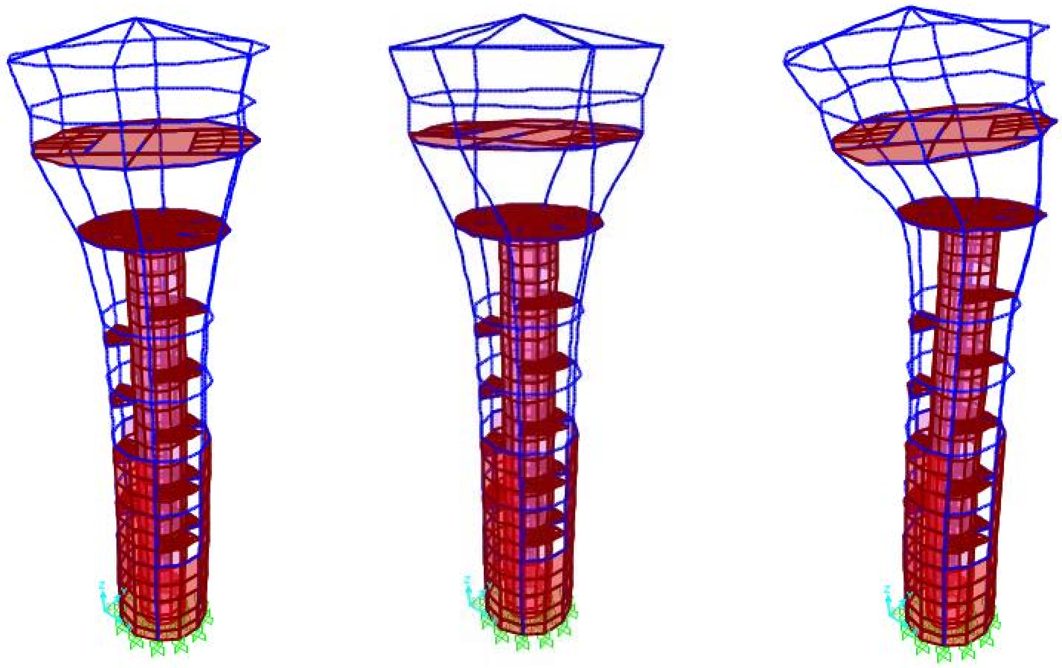

(a) First mode shape (b) Third mode shape (c) Fifth mode shape

Fig. 4 Mode shapes of the tower

3.2 Selected earthquake records

Selection of earthquake records has a significant impact on the obtained results from nonlinear time history analysis. Building codes normally limits the minimum number of earthquake records used for the time history analysis to three records while recommending the usage of 7 records. In this study, 14 earthquake records were selected for nonlinear time history analyses that can be categorized into seven near-field and seven far-filed records. The records were selected from the Pacific Earthquake Engineering Research Centre (PEER 2009) database. Since the average shear wave velocity of the construction site was less than 175 m/s, only recorded accelerations on the soil class D of United State Geological Survey (USGS) were selected. In addition to the soil class and source-to-site distance, special attention was paid to the Peak Ground Acceleration (PGA) to Peak Ground Velocity (PGV) ratio of selected records. It has been demonstrated that PGA/PGV ratio provides useful information about the relative frequency content and duration of earthquake records and it correlates well with the magnitude and epicentral distance relationship associated with motions. (Tso *et al*. 1992, Dicleli and Bruneau 1995).

The selected records are shown in Table 7. The first seven earthquake records are the near-field records and the rest are the far-field records. It is evident that the selected records cover a vast range of PGA/PGV ratios. Fig. 5 shows the response spectra of the selected records along with site-specific hazard response spectrum for 10% probability of exceeding in 50 years that is used for the design of tower. Earthquake records were scaled before use in the nonlinear time history analysis. The proposed method by Eurocode 8 (EC8 2004) was adopted for scaling the selected records. In this method, the mean values of 5% damped elastic spectrum calculated from all time histories should not be less than 90% of the corresponding values of the code elastic response spectrum for periods ranging from 0.2T1 and 2T1, where T1 is the fundamental period of the structure. Fig. 6 depicts the spectral accelerations of scaled records along with the target spectrum.

Table 7 Properties of selected earthquake records

Name	Year	Station	Duration	PGA (g)	PGV (cm/s)	PGA/PGV
SUPERST/B-PTS	1987	Parachute Test Site	22	0.42	159.53	2.58
CHICHI/TCU065	1999	TCU065	90	0.82	146.10	5.54
NORTHR/SCS	1994	Sylmar - Converter Sta	40	0.80	93.30	8.36
IMPVALL/H-E07	1979	El Centro Array #7	37	0.46	188.49	2.41
ERZIKAN/ERZ	1992	Erzincan	21	0.49	142.68	3.36
CHICHI/CHY101	1999	CHY101	90	0.38	180.40	2.06
DENALI/ps10	2002	TAPS Pump Station #10	90	0.27	246.41	1.09
CHICHI/CHY067	1999	CHY067	208	0.06	84.62	0.67
CHICHI/CHY017	1999	CHY017	150	0.06	201.41	0.28
CHICHI/CHY090	1999	CHY090	90	0.08	135.07	0.56
LANDERS/HOS	1992	San Bernardino - E & Hospitality	120	0.09	91.52	0.93
CHICHI/CHY059	1999	CHY059	90	0.05	181.95	0.29
KERN/PEL	1952	LA - Hollywood Stor FF	70	0.06	70.47	0.79
LANDERS/COM	1992	Hacienda Heights - Colima	63	0.06	88.67	0.65

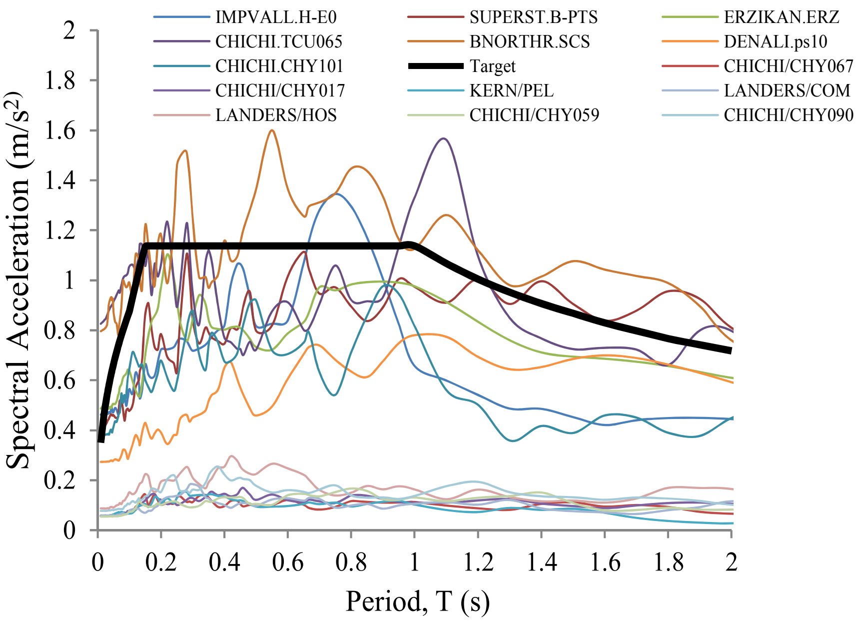

Fig. 5 Response spectra of selected records along with target response spectrum

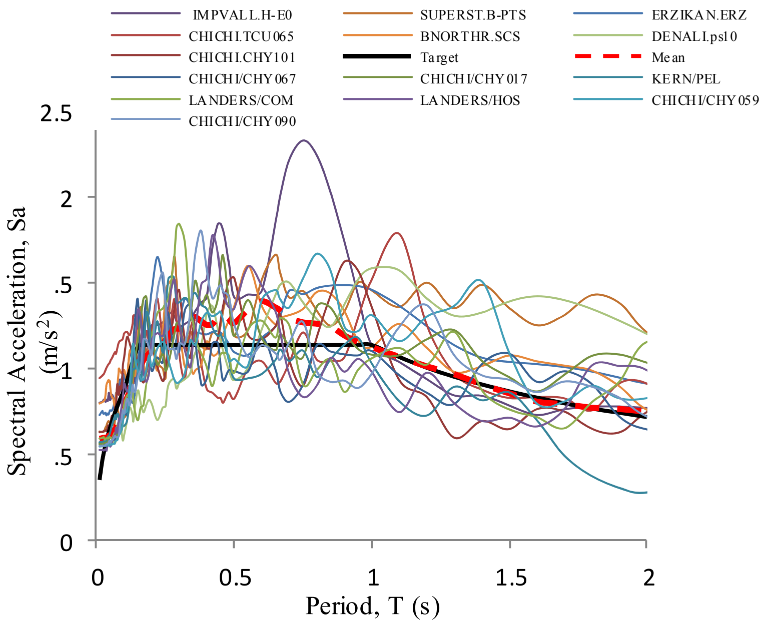

Fig. 6 Scaled response spectra of selected earthquake records

4. Results and discussion

4.1 Seismic design of the tower

The selected tower has been designed for seismic loads according to Iranian Code of Practice for Seismic Resistant Design of Buildings (ICPSRD 2005). In ICPSRD, seismic base shear (V) should be calculated through the equivalent static method using Eq. (8). In this equation "C" stands for seismic response coefficient and "W" is the effective seismic weight. "C" should be calculated using Eq. (9) in which "A" is the design base acceleration for the construction site, "I" is the importance factor, "R" is the response modification factor and B is the reflection coefficient. According to the seismic hazard map of ICPSRD for the design basis earthquake at the construction site of this tower, A=0.25 g. In addition, for ATC towers, ICPSRD recommends, I=1.4. Similar to other seismic codes like ASCE/SEI 7-10 (2010), the "R" factor in ICPSRD accounts for the ductility of structures and adjust the design seismic loads accordingly. According to ICPSRD for structures that have different lateral load resistance systems along their height, the value of R should be taken as the least of recommended values for the lateral load resistance systems employed in the structure. In this tower, the lateral load resistance system before reaching to the level of equipment room is a dual system (concrete core combined with MRF), however, after this level the tower relies only on the MRF. The recommended R-factor for the dual system in ICPSRD is R=8 while for the MRF is R=7. Therefore, following the requirement of ICPSRD for the design of this tower value of R is taken 7.

Eqs. (10) to (12) define the reflection factor which accounts for soil effects. T0, TS, and S in these equations should be obtained from a table provided in ICPSRD. For the tower under investigation since the average shear wave velocity is less than 175 m/s, T0=0.15, TS=1 and S=2.25. According to ICPSRD, for non-building structures (like this tower) the ratio of B/R should not be considered less than 0.5, therefore, by substituting the given values into the given equations the seismic response coefficient can be calculated as C=0.175. This value implies that the design seismic base shear for this tower equals to 17.5% of its seismic weight. It should be noted that, the applied limitation on the B/R ratio has only increased the value of seismic base shear coefficient 8% in comparison to the buildings that have similar structural system and the fundamental natural frequency. For vertical distribution of the seismic base shear obtained from equivalent static method, ICPSRD employs similar approach to that of Uniform Building Code (UBC 1997).

$$V=C.W \tag{8}$$

$$C=A.B.I/R \tag{9}$$

$$B = 1 + S\left(\frac{T}{T_0}\right) \qquad \textit{If} \quad 0 \le T \le T_0 \tag{10}$$

$$B = 1 + S \qquad \textit{If} \quad T_0 \le T \le T_S \tag{11}$$

$$B = (S+1)\left(\frac{T_S}{T}\right)^{2/3} \qquad \textit{If} \quad T \ge T_S \tag{12}$$

In ICPSRD, response spectrum analysis should be employed together with the equivalent static method when analyzing non-building structures having a fundamental period more than 0.5 sec. The 5% damped response spectrum used for the seismic design of this tower is shown in Figs. 5 and 4. It should be mentioned that, according to ICPSRD the seismic base shear obtained from response spectrum analysis should not be less 80% of equivalent static method (Eq. (1)) for regular structures and 100% of it for irregular structures. For the studied tower, since the obtained seismic base shear from response spectrum method was less than that of equivalent static method, it was modified accordingly. Fig. 7 displays shear force distribution along the height of tower using equivalent static method and response spectrum analysis. It is seen that response spectrum analysis predicts more shear forces at higher levels especially at the level of equipment room where the tower relies only on the MRF. It should be noted that the seismic base shear obtained from both linear methods are equal at the foundation level as specified by ICPSRD. Fig. 8 compares drift ratios along the height of the tower. Although at lower levels the differences between results of these two methods are negligible, a significant difference at the level of equipment room can be observed. This significant difference relies on the fact that the equivalent static method only considers the first mode of vibration for seismic analysis. However, as it was observed from Fig. 4, the fifth mode shape had a great impact on the dynamic behavior of the tower. Since the first 35 mode shapes of the tower were included in the response spectrum analysis, this method reflected the inter-story drift demands at higher levels much better than equivalent static approach. According to ICPSRD, for buildings with a fundamental period of less than 0.7 s the inter-story elastic drift ratios should not exceed 0.025/0.7R which equals to 0.005 for this tower. As can be seen from Fig. 8, the drift value at the equipment room reaches to 0.0076 which is 1.5 times more than the code specified limitation for buildings. ICPSRD does not impose the drift limitation on non-building structures unless damage to non-structural components can lead to fatality. Records from past earthquakes have offered that extra attention is needed for non-structural parts of ATC towers to preserve communication systems active. Destruction to nonstructural components can

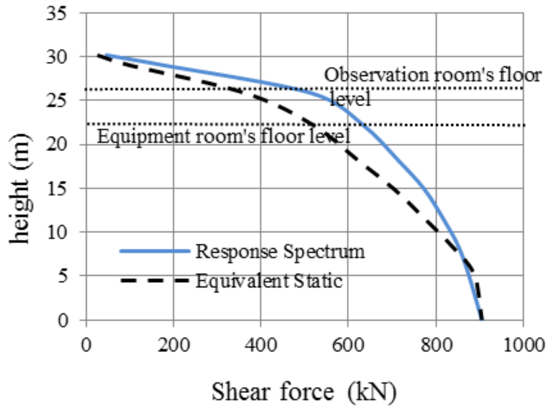

Fig. 7 Shear force distribution along the height of tower

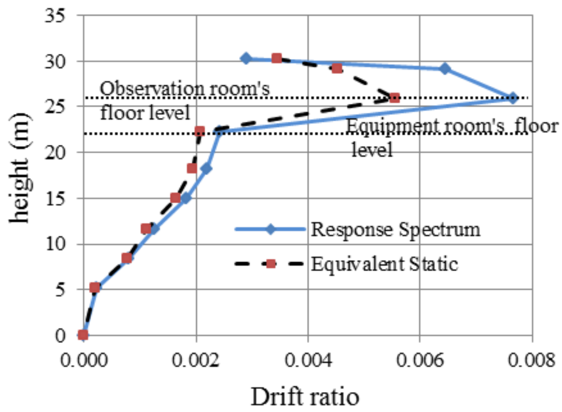

Fig. 8 Drift ratios along the height of tower

interrupt data transferring and definitely stop working of ATC towers which was found by Pierepiekarz *et al*. (2001). Considering this fact that the observation and equipment rooms are occupied by sensitive devices, the ICPSRD drift limitation should be considered in the design of ATC towers.

4.2 Results of nonlinear time history analysis

Nonlinear time history analysis is considered to be the most accurate method in order to estimate seismic demands of structures subjected to ground motions. In this study, the tower was excited by the 14 scaled earthquake records and structural responses were recorded. Fig. 9 shows the mean of shear forces obtained from Nonlinear Time History (NTH) analysis and compares them with those values obtained by Equivalent Static (ES) method and Response Spectrum (RS) analysis. It is seen that the base shear from NTH analysis is 3.6 times greater than that of ES method. However, as the height of tower increases the difference in shear forces reduces until at the level of observation room, NTH analysis predicts slightly lower shear forces compared to RS and ES approaches. The reason for the significant difference in the base shears obtained from linear and NTH analyses lies on this fact that in linear analysis, unlike NTH analysis, seismic actions are reduced by the R-factor in order to indirectly account for the ductility and energy dissipation capacity of structural components. It should be mentioned that, the additional base shears obtained from NTH analysis result in inelastic deformation in structural components which has been discussed in the subsequent sections.

Fig. 10 compares the mean inelastic drift ratios obtained from NTH analyses with those obtained from linear methods. It is evident that the mean inelastic drift ratios follow a similar pattern to that of linear methods. However, NTH analysis predicts significantly higher drift ratios in comparison to the linear analyses. By comparing elastic and inelastic drift ratios obtained from linear and nonlinear analyses a displacement amplification factor (C_d) of 2.6 can be obtained for the equipment room. This value is lower than what building codes recommend for steel MRF with a medium class of ductility (e.g., C_d=4 in ASCE/SEI 7-10). For buildings, ICPSRD recommends that the C_d should be taken as 0.7R in order to estimate the inelastic drift ratio. As can be seen from Fig. 10, there is a close agreement between results of NTH analysis and predictions of ICPSRD for lower levels of the tower. However, ICPSRD significantly overestimates the inelastic drift ratio at the roof level of the equipment room. This problem is mostly attributed to the recommended displacement amplification factor by ICPSRD. Since the tower along the height take advantage of two different lateral load resisting systems, use of only one displacement amplification factor for the entire height may not reflect the inelastic dynamic behavior of the tower properly.

Fig. 11 displays the obtained overturning moments along the height of the tower. At the base, NTH analysis predicts overturning moment which is almost 3 times more than RS analysis and ES method. However, the difference between obtained results decreases as the height increases. It is seen that, all analyzing methods estimate almost similar over turning moment for the level of observation room which agrees well with obtained results for shear force and drift ratios. The obtained over turning moment at the base of tower indicates that the factor of safety against overturning for the tower should be considered greater than common values recommended by

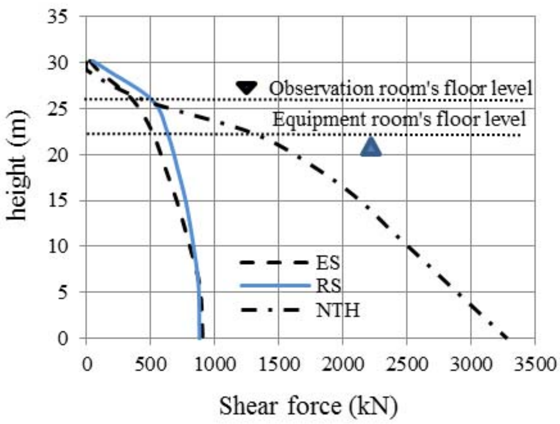

Fig. 9 Comparison of Shear force distribution along the height of tower

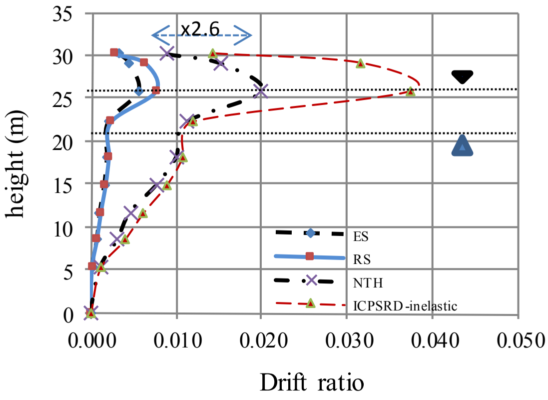

Fig. 10 Comparison of drift ratio along the height of the tower

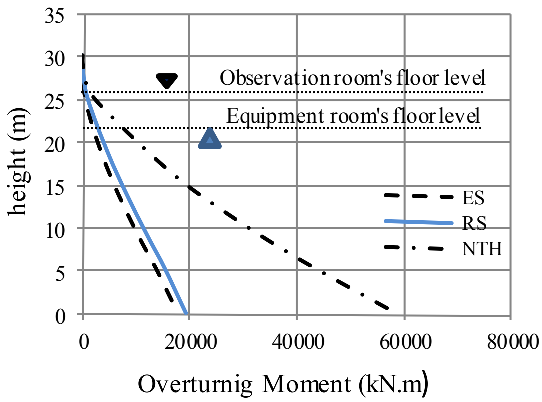

Fig. 11 Comparison of overturning moment along the height of the tower

building codes (e.g., 1.5 ~1.75). It should be noted that the difference between the mean of maximum structural responses obtained from far-field and near-field records was less 20%. Therefore, only the mean of maximum responses obtained for all 14 records was presented in the figures.

4.2.1 Shear force distribution between walls and frame

It is of great interest to study shear force distribution among concrete walls and steel MRF using different analyzing methods. As Fig. 12 indicates, NTH analysis estimates that the maximum shear force for the MRF occurs at the height of 22.2 m where the inner concrete core is finished. However, results of ES and RS analyses shows that the maximum shear force for MRF occurs at the height of 11.7 m where the outer concrete core is finished. Results of response spectrum analysis also show that, the MRF between 6 m to 9 m height does not participate in shear force absorption and leans on concrete cores. Fig. 13 shows that, although the intensity of shear forces obtained from NTH analysis are significantly more than linear analyses, all methods estimate a similar pattern for shear force distribution in the outer concrete cores. As can be seen from Fig. 14, results of ES and RS analyses display that the inner core has a negligible role in absorbing shear forces between 5 m to 8 m height and the maximum shear force in the inner core occurs at the base of tower. However, NTH analysis shows that the inner core reaches to its maximum shear force at 12 m height and contributes to shear force absorption all along the height of tower. Linear and nonlinear methods agree that the outer concrete core absorbs shear forces more than the MRF and inner core between foundation level and 10 m height. However, from 12 m to 20 m height, NTH analysis estimates more shear forces for the inner concrete core compared to the MRF which is in contradiction to what linear analyses predict.

It is worth mentioning that, the inelastic behavior of concrete walls was also simulated by discrete plastic hinge method. The concrete walls were divide into small elements each of which having 2 m height. The mass of each element was calculated and lumped at the end of element. Plastic hinges were modeled using yield and ultimate moment capacities calculated for each element. For each element one plastic hinge was assigned to its end. The plastic hinge length was considered to be 20% of the concrete core's diameter (Wilson 2002). The failure criterion for each element was based on curvature demand predicted from NTH analysis reaching to the curvature capacity of each element. The compressive and tensile strains used for the calculation of curvature capacities, followed the given values in Table 5. Meanwhile, the modified Takeda model was selected to represent the hysteretic behavior of plastic hinges. The effective stiffness of concrete walls was considered to be $0.5EI_g$ in which E and I_g stand for modulus of elasticity and gross cross section's moment of inertia, respectively (ATC40 1996, Paulay and Priestley 1992). In general, obtained results from fiber and discrete hinge methods were in close agreement in a sense that similar patterns were observed for shear force and bending moment distributions along the height of the tower. However, the median of maximum shear force and bending moment demands obtained from discreet hinge method were slightly (around 15%) more than that of fiber method. Such difference is due to this fact that the fiber method ignored the tensile strength of concrete and tension stiffening effect, therefore, resulting in a more flexible structure compared to the discrete hinge method.

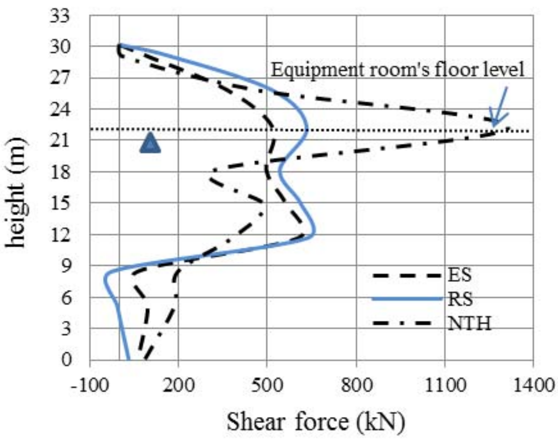

Fig. 12 Shear force absorbed by the steel MRF

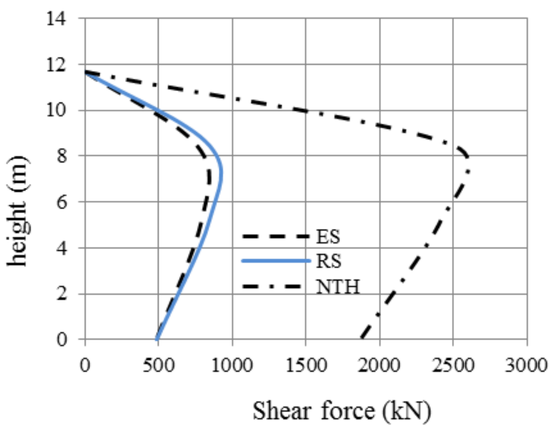

Fig. 13 Shear force absorbed by the outer concrete core

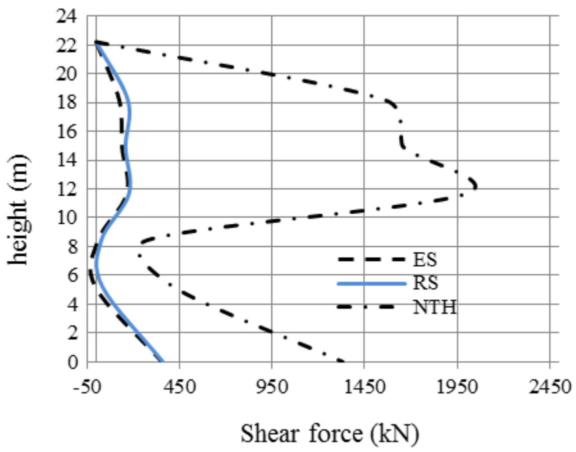

Fig. 14 Shear force absorbed by the inner concrete core

4.2.2 Performance-Based seismic design of the tower

Vafaei *et al*. (2013) concluded the PBSD of structures is the seismic design practice that lets structural engineers to decide appropriate levels of ground motion and performance goals for structural and non-structural part of a structure in order to survive specific seismic behaviors. By using this technique, a structure can be designed for a series of performance levels when subjected to different levels of seismic hazards. As a result, PBSD provides a better solution than building codes for the seismic design of ATC towers.

Often, when structures are designed according to building codes, they are expected to satisfy life safety performance level when seismic hazard is set to the Design Basis Earthquake (DBE). ICPSRD specifies that Immediate Occupancy (IO) level can be expected for very important buildings (Importance factor=1.4) that are designed according to this code when seismic hazard is set to DBE. In order to evaluate the seismic performance level of the tower, plastic hinge formations and yielding of reinforcements were monitored during seismic excitations. Fig. 15(a) displays the envelope of obtained results for plastic hinge formations in MRF when seismic hazard level was set to DBE (PGA=0.3 g). As can be seen from this figure, all plastic hinges remain in IO level indicating that the MRF complies with the requirement of IO level. It would be of great interest to evaluate the seismic performance of MRF when it is subjected to the seismic hazard at MCE level. For the tower under consideration the Peak Ground Acceleration (PGA) at MCE level is PGA=0.4 g. Fig. 15(b) displays plastic hinge formations at MCE level. It is seen that, plastic hinges mostly form at circular beams and they pass Collapse Prevention (CP) level indicating that for very severe earthquakes the MRF does not satisfy collapse prevention performance level. Although, ICPSRD does not consider the CP performance level for the design of buildings, ATC towers are expected to comply with the requirements of collapse prevention performance level when the seismic hazard is set to MCE (Muthukumar and Sabelli 2013). Fig. 15(b) also shows that, unlike DBE level, plastic hinges form in columns when the intensity of earthquakes increases. However, as it was expected from the results of overturning moments, columns at the level of observation room still remain in elastic range. It should be noted that, absence of CP performance level in the plastic hinge of MRF columns is because of major contribution of concrete cores in shear force absorption as it was discussed in the previous section.

Envelopes of stress intensities in the longitudinal reinforcements of concrete cores are presented in Figs. 16(a), (b). Considering the yield stress of reinforcements used in the design, F_y=400 N/mm^2, it can be observed that longitudinal reinforcements in both inner and outer cores have reached to the yield stress. For the outer core, yielding has occurred locally at the corner of concrete walls where steel columns connect to concrete core through shear connectors. However, yielding in the inner core's reinforcements has occurred almost at its mid height where the outer core reaches to its end and shear forces should be only carried by MRF and inner core. It should be noted that, results of shear force distributions along the height of tower shown in Figs. 13 and 15 correlates well with the obtained results for yielding of reinforcements. This is evident that, unlike

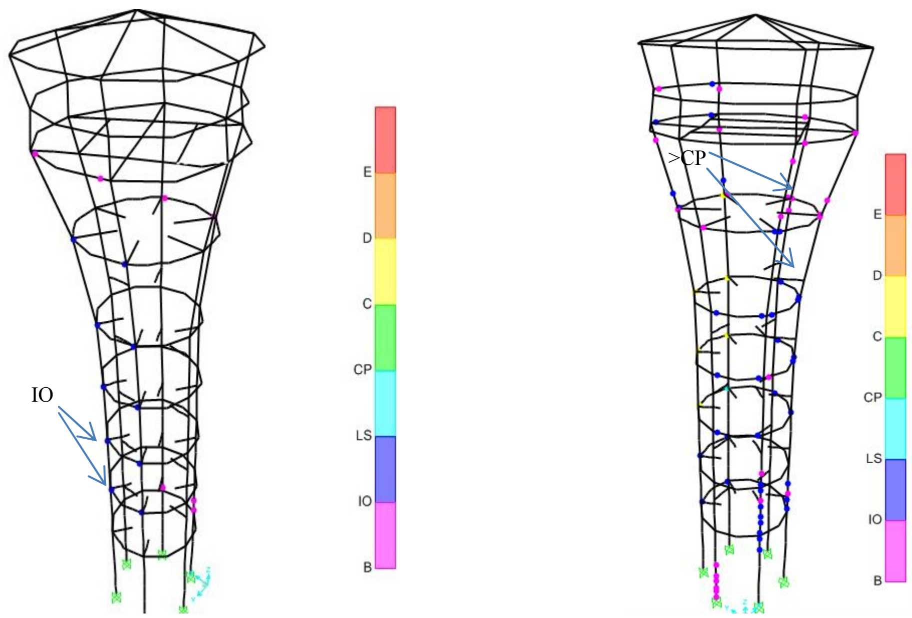

(a) DBE level (b) MCE level

Fig. 15 Plastic hinge formations in the MRF

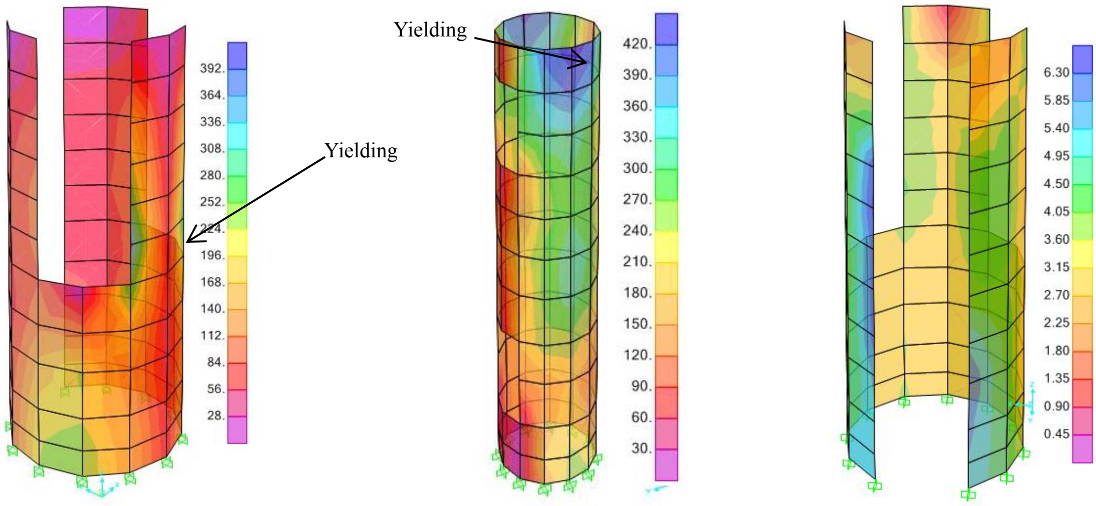

(a) Stress in longitudinal reinforcements of outer core

(b) Stress in longitudinal reinforcements of inner core

(c) Stress in concrete of outer core

Fig. 16 Envelope of stress intensities obtained for concrete cores at DBE level (N/mm^2)

the MRF, concrete cores did not satisfy the IO performance level as it was required by ICPSRD for very important structures. It is worth mentioning that, the obtained compressive stress in the concrete of both inner and outer cores was less than 30% of ultimate compressive strength considered in the design (28 N/mm2). Therefore, unlike the stress level in reinforcements, the maximum stress level in the concrete of shear walls comply with the IO performance level.

Although the observed failure mechanisms (plastic hinge formation in beams and yielding of reinforcements in concrete cores) are considered to be desirable for a ductile seismic behavior, the studied tower that is designed and detailed according to specifications of a building code (ICPSRD) through linear static and dynamic analyses does not satisfy the expected seismic performance levels. This indicates that, for seismic design and evaluation of ATC towers a more sophisticated approach rather than building codes should be employed. Performance-based seismic design can be a promising technique for this purpose.

5. Conclusions

Seismic performance of an existing ATC tower with wall-frame structural system and total height of 30.1m that was designed and detailed according to specifications of a building code (ICPSRD) was evaluated through nonlinear time history analysis. Immediate occupancy performance level when seismic hazard was set to DBE level together with collapse prevention performance level when seismic hazard was set to MCE level were considered as seismic performance objectives. It was observed that the moment resistance frame of the tower complied well with the requirements of IO level; however, it failed to satisfy requirements of collapse prevention level. Concrete cores failed to satisfy requirements of IO level because of yielding of reinforcements. Failure mechanism of the tower was plastic hinge formation in beams along with yielding of reinforcements in inner and outer concrete cores. The maximum compressive stress in the concrete of shear walls was less than 30% of ultimate concrete strength used for the design of tower. The proposed method by the building code overestimated the maximum inelastic drift ratio that occurred at the level of equipment room. Based on the results of nonlinear time history analysis, displacement amplification factor was estimated to be 2.6 for the tower under consideration. Results of nonlinear time history analysis indicated that, linear analyzing methods used in the design of tower are incapable of proper shear force distribution between concrete cores and steel moment resistance frame. It was concluded that, for a safe seismic design of ATC tower practice engineers should rely on more sophisticated methods like Performance-Based seismic design.

References

AISC-ASD89 (1989), *Allowable Stress Design and Plastic Design Specifications for Structural Steel Buildings*, American Institute of Steel Construction, Chicago, Illinois.

Al-Bermani, F.G. and Kitipornchai, S. (1990), "Elasto-plastic large deformation analysis of thin-walled structures", *Eng. Struct.*, **12**(1), 28-36.

Aman, M., Nadeem, H. and Khaled, E.S. (2015), "Seismic performance and cost-effectiveness of high-rise buildings with increasing concrete strength", *Struct. Des. Tall Spec. Build.*, **24**(4), 257-279.

American Concrete Institute (ACI) Committee 318 (1999), Building Code Requirements for Reinforced Concrete and Commentary (ACI 318-99/ACI 318R-99*)*, Farmington Hills, MI.

American Society of Civil Engineers (ASCE) (2010), "Minimum design loads for buildings and other structures", *ASCE/SEI 7-10*, ASCE, Reston, VA.

ATC 40 (1996), *Seismic evaluation and retrofit of concrete buildings*, Applied Technology Council, CA.

Chan, S.L. and Zhou, Z.H. (1998), "On the development of a robust element for second-ordernon-linear integrated design and analysis (nida)", *J. Constr. Steel Res.*, **47**(1), 169-190.

Chen, X.W., Li, J.X. and Cheang, J. (2010), "Seismic performance analysis of Wenchuan Hospital structure with viscous dampers", *Struct. Des. Tall Spec. Build.*, **19**(4), 397-419.

Değer, Z.T., Yang, T.Y., Wallace, J.W. and Moehle, J. (2015), "Seismic performance of reinforced concrete core wall buildings with and without moment resisting frames", *Struct. Des. Tall Spec. Build.*, **24**(7), 477-490.

Dicleli, M. and Bruneau, M. (1995), "Seismic performance of multispan simply supported slab-on-girder steel highway bridges", *Eng. Struct.*, **17**(1), 4-14.

Eshghi, S. and Farrokhi, H. (2003), "Seismic vulnerability analysis of airport traffic control towers", *J. Seismol. Earthq. Eng.*, **5**(1), 31.

Eurocode 8 (2004), *Design of structures for earthquake resistance*, Part 1, 1998-1.

Federal Emergency Management Association (2000), *Prestandard and commentary for the seismic rehabilitation of buildings*, American Society of Civil Engineers (ASCE).

Foley, C.M. and Vinnakota, S. (1999), "Inelastic behavior of multistory partially restrained steel frames. Part II", *J. Struct. Eng.*, **125**(8), 862-869.

Goyal, A. and Maiti, M.K. (1997), "Inelastic seismic resistance of reinforced concrete stack-like structures", *Earthq. Eng. Struct. Dyn.*, **26**(5), 501-513.

ISO 690 Iranian Code of Practice for Seismic Resistant Design of Buildings (2005), *Standard No. 2800, 3rd edition*, Building & Housing Research Center, Tehran, Iran.

Izzuddin, B.A. and Smith, D.L. (1996), "Large-displacement analysis of elastoplastic thin-walled frames. I: formulation and implementation", *J. Struct. Eng.*, **122**(8), 905-914.

Jiang, X.M., Chen, H. and Liew, J.R. (2002), "Spread-of-plasticity analysis of three-dimensional steel frames", *J. Constr. Steel Res.*, **58**(2), 193-212.

Kim, S.E., Park, M.H. and Choi, S.H. (2001), "Direct design of three-dimensional frames using practical advanced analysis", *Eng. Struct.*, **23**(11), 1491-1502.

Kitipornchai, S., Al-Bermani, F.G.A. and Chan, S.L. (1988), "Geometric and material nonlinear analysis of structures comprising rectangular hollow sections", *Eng. Struct.*, **10**(1), 13-23.

Li, G., Zhang, F., Zhang, Y. and Li, H.N. (2015), "Nonlinear hysteretic behavior simulation of reinforced concrete shear walls using the force analogy method", *Struct. Des. Tall Spec. Build.*, **24**(7), 504-520.

Li, W., Li, Q.N. and Jiang, W.S. (2013), "Nonlinear finite element analysis of behaviors of steel beam-continuous compound spiral stirrups reinforced concrete column frame structures", *Struct. Des. Tall Spec. Build.*, **22**(15), 1119-1138.

Liew, J.R., Chen, H., Shanmugam, N.E. and Chen, W.F. (2000), "Improved nonlinear plastic hinge analysis of space frame structures", *Eng. Struct.*, **22**(10), 1324-1338.

McKenna, F., Fenves, G.L. and Scott, M.H. (2000), "Open system for earthquake engineering simulation", University of California, Berkeley, CA.

Muthukumar, S. and Sabelli, R. (2013), "Nonlinear seismic analysis of a round concrete tower with a post-tensioned self-centering system", *Structures Congress 2013 sBridging Your Passion with Your Profession*, ASCE.

Orakcal, K., Wallace, J.W. and Conte, J.P. (2004), "Flexural modeling of reinforced concrete walls-model attributes", *ACI Struct. J.*, **101**(5), 688-698.

Panneton, M., Léger, P. and Tremblay, R. (2006), "Inelastic analysis of a reinforced concrete shear wall building according to the National Building Code of Canada 2005", *Can. J. Civ. Eng.*, **33**(7), 854-871.

Paulay, T. and Priestley, M.J.N. (1992), *Seismic design of reinforced concrete and masonry buildings*, New York: Wiley.

Pi, Y.L. and Trahair, N.S. (1994), "Nonlinear inelastic analysis of steel beam-columns. I: Theory", *J. Struct. Eng.*, **120**(7), 2041-2061.

Pierepiekarz, M.R., Ballantyne, D.B. and Hamburger, R.O. (2001), "Damage report from Seattle", *Civ. Eng.*, **71**(6), 78.

Rad, B.R. and Adebar, P. (2009), "Seismic design of high-rise concrete walls: reverse shear due to diaphragms below flexural hinge", *J. Struct. Eng.*, **135**(8), 916-924.

Roark, M.S., Turner, K.Z. and Gould, P.L. (2000), "Seismic vulnerability of airport facilities", MSc. Thesis, Washington University.

SAP2000 V15 (2013), Integrated Software for Structural Analysis & Design. Computers & Structures, Inc., Berkeley, California, USA.

Shahidi, F., Rezaeian, A., Jamal-Omidi, M. and Shahidi, F. (2015), "Investigation of the ConXL moment connection cyclic behavior in box columns without filling concrete with different arrangement of collar bolts", *Struct. Des. Tall Spec. Build.*, **24**(5), 317-350.

Teh, L.H. and Clarke, M.J. (1999), "Plastic-zone analysis of 3D steel frames using beam elements", *J. Struct. Eng.*, **125**(11), 1328-1337.

Tso, W.K., Zhu, T.J. and Heidebrecht, A.C. (1992), "Engineering implication of ground motion A/V ratio", *Soil Dyn. Earthq. Eng.*, **11**(3), 133-144.

U.B. Code (1997), *BC-97*, American Association of Building Officials, Whittier, CA.

Vafaei, M., Adnan, A.B. and Rahman, A.B.A. (2014), "Seismic performance evaluation of an airport traffic control tower through linear and nonlinear analysis", *Struct. Infra. Eng.*, **10**(8), 963-975.

Wilcoski, J. and Heymsfield, E. (2002), "Performance and rehabilitation of type L FAA airport traffic control tower at San Carlos, California, for seismic loading", *J. Perform. Constr. Facil.*, **16**(2), 85-93.

Wilson, J.L. (2003), "Earthquake response of tall reinforced concrete chimneys", *Eng. Struct.*, **25**(1), 11-24.

Zekioglu, A., Willford, M., Jin, L. and Melek, M. (2007), "Case study using the Los Angeles tall buildings structural design council guidelines: 40-storey concrete core wall building", *Struct. Des. Tall Spec. Build.*, **16**(5), 583-597.

KT